An engineered minimal chromosomal passenger complex reveals a role for INCENP/Sli15 spindle association in chromosome biorientation

Sarah Fink,[1] Kira Turnbull,[2,3] Arshad Desai,[2,3] and Christopher S. Campbell[1]

[1]Department of Chromosome Biology, Max F. Perutz Laboratories, University of Vienna, 1030 Vienna, Austria
[2]Ludwig Institute for Cancer Research and [3]Department of Cellular and Molecular Medicine, University of California, San Diego, La Jolla, CA 92093

The four-subunit chromosomal passenger complex (CPC), whose enzymatic subunit is Aurora B kinase, promotes chromosome biorientation by detaching incorrect kinetochore–microtubule attachments. In this study, we use a combination of truncations and artificial dimerization in budding yeast to define the minimal CPC elements essential for its biorientation function. We engineered a minimal CPC comprised of the dimerized last third of the kinase-activating Sli15/INCENP scaffold and the catalytic subunit Ipl1/Aurora B. Although native Sli15 is not oligomeric, artificial dimerization suppressed the biorientation defect and lethality associated with deletion of a majority of its microtubule-binding domain. Dimerization did not act through a physical clustering-based kinase activation mechanism but instead promoted spindle association, likely via a putative helical domain in Sli15 that is essential even when dimerized and is required to target kinetochore substrates. Based on the engineering and characterization of a minimal CPC, we suggest that spindle association is important for active Ipl1/Aurora B complexes to preferentially destabilize misattached kinetochores.

Introduction

In eukaryotes, accurate segregation of the genetic material requires the products of DNA replication, paired sister chromatids, to connect with the correct geometry to spindle microtubules. Each chromatid must attach exclusively to microtubules from one spindle pole, and the two identical chromatids of a pair must connect to opposite poles. Erroneous connections that form on the path to this bioriented state are corrected by the kinase Aurora B. Aurora B phosphorylation of kinetochores lowers their affinity for microtubules, increasing turnover of kinetochore–microtubule attachments (Tanaka et al., 2002; Cheeseman et al., 2006; Sarangapani et al., 2013; Kalantzaki et al., 2015), which improves the likelihood that all chromosomes achieve the correct bioriented state (Lampson et al., 2004; Cimini et al., 2006). The budding yeast *Saccharomyces cerevisiae* is an important model to understand the mechanism of Aurora B action, as inhibition of Aurora B (Ipl1) in this species leads to very high (>90%) missegregation that arises from the inability to correct syntelic kinetochore–microtubule attachments, wherein the kinetochores of sister chromatids are attached to the same spindle pole (Biggins and Murray, 2001; Tanaka et al., 2002; Pinsky et al., 2006).

Aurora B/Ipl1 is a member of the four-subunit chromosomal passenger complex (CPC), along with Sli15/INCENP, Bir1/Survivin, and Nbl1/Borealin. The CPC has two conserved localizations: on chromatin and on microtubules (Cooke et al., 1987). In prometaphase and metaphase, the complex primarily localizes to chromatin at the inner centromere through either the Borealin or Survivin subunits, which form a three-helix bundle with the N-terminal CEN box of INCENP (Jeyaprakash et al., 2007; Kelly et al., 2010; Wang et al., 2010; Yamagishi et al., 2010; Cho and Harrison, 2011). Although in fission yeast and cancer cell lines, perturbation of the inner centromeric localization of the CPC results in misalignment and missegregation of chromosomes (Dai et al., 2005; Vader et al., 2006; Yamagishi et al., 2010), in chicken DT40 cells and in budding yeast, mutations that mislocalize the CPC away from the inner centromere are viable and do not exhibit significant chromosome missegregation (Yue et al., 2008; Campbell and Desai, 2013). In budding yeast, disruption of centromere localization is synthetic lethal with mutations affecting centromeric cohesion, suggesting that this localization may be relevant for a nonessential function in chromatid cohesion at centromeres (Campbell and Desai, 2013).

At anaphase onset, the CPC transitions to the microtubules between the separating chromatids. This localization relies on the central region of INCENP. Although the sequence is not well conserved, a coiled-coil is predicted in this region of INCENP from different species (Mackay et al., 1993; van der Horst and Lens, 2013). Although initially expected to be a coiled-coil, this

Correspondence to Christopher S. Campbell: christopher.campbell@univie.ac.at; or Arshad Desai: abdesai@ucsd.edu

Abbreviations used: CPC, chromosomal passenger complex; FRB, FKBP–Rapamycin binding; PR, phosphoregulated; SAH, single α helix.

The Rockefeller University Press $30.00
J. Cell Biol. Vol. 216 No. 4 911–923
https://doi.org/10.1083/jcb.201609123

region was later predicted to instead be a single α helix (SAH) that does not oligomerize (Peckham and Knight, 2009), and this prediction was subsequently verified (Samejima et al., 2015). The INCENP SAH binds directly to microtubules in vitro and the interaction requires positively charged residues of the predicted helix (Samejima et al., 2015; van der Horst et al., 2015).

The *S. cerevisiae* INCENP, Sli15, has a region adjacent to its putative SAH region (based on coiled-coil predictions), which is phosphorylated by both Cdk1/Cdc28 and Aurora B/Ipl1 and is dephosphorylated by the phosphatase Cdc14 at anaphase onset. We name this region, which has no structured domains, the phosphoregulated (PR) region (Fig. 1 A). Preventing Sli15 phosphorylation in this region causes it to localize prematurely to spindle microtubules in metaphase, demonstrating that dephosphorylation of this region regulates the transition to microtubules in anaphase. Nonphosphorylatable mutants of the PR region decrease the rate of anaphase spindle elongation but do not otherwise affect growth or viability (Pereira and Schiebel, 2003; Nakajima et al., 2011; Makrantoni et al., 2014). In contrast, deletions within the PR region are lethal and result in high chromosome missegregation rates (Sandall et al., 2006; Campbell and Desai, 2013).

At the C terminus of INCENP, distal to the SAH, is the conserved IN box that binds to and activates Aurora B kinase (Sessa et al., 2005). Aurora B is also activated by physical clustering of the CPC, e.g., by localization to the microtubule surface or by antibody-mediated cross-linking, which promotes transphosphorylation of neighboring molecules (Kelly et al., 2007; Tseng et al., 2010). We previously showed that a Sli15 deletion mutant that prevents localization to the inner centromere leads to both its and Ipl1's increased enrichment on metaphase spindles, which led to the model that kinase activation by clustering on microtubules was sufficient for chromosome biorientation in the absence of inner centromere localization (Campbell and Desai, 2013).

In this study, to test the clustering-based kinase activation model for the role of microtubule binding by Sli15, we used truncations and artificial dimerization to engineer a minimal CPC, comprised of Ipl1 and a dimerized SAH–IN box segment of Sli15, that we show is sufficient for the CPC's essential biorientation function. Although dimerization compensated for the removal of the PR region of Sli15, it did not compensate for removal of the putative SAH. Notably, analysis of the minimal CPC that requires dimerization for function did not reveal a role for clustering-based kinase activation and instead suggested that spindle association, likely mediated by the SAH, is essential to target substrates at the kinetochore in order to correct misattachments and promote biorientation.

Results

The PR region of the Sli15 microtubule-binding domain promotes chromosome segregation fidelity and is essential for viability

To determine whether specific parts of the PR region of Sli15 are required for chromosome segregation, we engineered sequential deletion constructs (Fig. 1 A). All five tested deletions, including the smallest deletion (Δ2–300) extending past the region previously demonstrated to be dispensable (Δ2–228; Campbell and Desai, 2013), resulted in lethality, as assayed by the inability of mutant spores to form colonies after tetrad dissection (Fig. 1 A). Immunoblots using an antibody raised against the C terminus of Sli15 showed that the truncated constructs were expressed at levels equal to or greater than endogenous Sli15 (Fig. 1 B). A construct that deletes only the PR region (*Δ228–450*) was also lethal, indicating that the lethality was not a synthetic effect of deleting both the PR region and the CEN box.

As biorientation is the only known essential function of the CPC in budding yeast, these results indicate that the PR region contributes to chromosome segregation. We tested this directly by monitoring the missegregation of chromosome IV in the first cell division after depletion of full-length Sli15 expressed under the control of a galactose-inducible promoter (Fig. 1 C). In the absence of any rescuing Sli15, the missegregation rate for chromosome IV was ∼60% per division. The Δ2–300 and Δ2–350 deletions resulted in missegregation rates of ∼5% for chromosome IV per division, which is consistent with the observed lethality. Larger deletions resulted in higher missegregation rates of ∼30% for the marked chromosome, indicating that these deletions were significantly compromised in their ability to correct syntelic kinetochore–microtubule attachments. Thus, the central PR region of Sli15 plays an essential role in chromosome segregation.

Artificial dimerization suppresses the biorientation defect and lethality associated with deletions within the Sli15 microtubule-binding domain

Based on the role of clustering in Aurora B kinase activation, a likely explanation for why deletions in the microtubule-binding region are lethal is that they limit kinase activation by reducing clustering on microtubules. To test this possibility, we artificially dimerized Sli15 through an N-terminal fusion with the obligate dimer GST. Addition of GST rescued the lethality of all of the PR region deletions (Fig. 2 A). Growth of even the largest deletion construct (GST-*Δ2–500*) was indistinguishable from full-length Sli15, as assayed by both colony size and dilution series on rich media (Fig. 2, A and B). When challenged with a moderate concentration of the microtubule-depolymerizing drug benomyl, only GST-*Δ2–500* displayed increased drug-sensitivity relative to full-length (Fig. 2 B). Direct measurement of chromosome missegregation revealed that fusion to GST lowered missegregation rates of PR region deletions to levels indistinguishable from GST-fused, full-length Sli15 (Fig. 2 C). Collectively, these results indicate that the essential function or functions of the PR region of Sli15 can be compensated for by fusion to the exogenous dimer, GST.

To test whether dimerization is the basis for the rescue of PR region deletion by GST fusion, we fused Sli15Δ2–450 to FKBP–Rapamycin binding (FRB) and FKBP12 domains, coexpressed the fusions in the same cell, and inducibly heterodimerized them by addition of the drug Rapamycin (Fig. 2 D). We observed a rescue of the lethality of Sli15Δ2–450 only in the presence of Rapamycin, providing strong support for the conclusion that dimerization is the property that rescues the lethality associated with the removal of the PR region. One explanation for rescue observed by GST fusion or inducible dimerization mediated by Rapamycin is that they compensate for dimerization mediated by the PR region. However, we were unable to detect association between coexpressed Venus- and 6HA-tagged Sli15 via immunoprecipitation from yeast extracts, suggesting

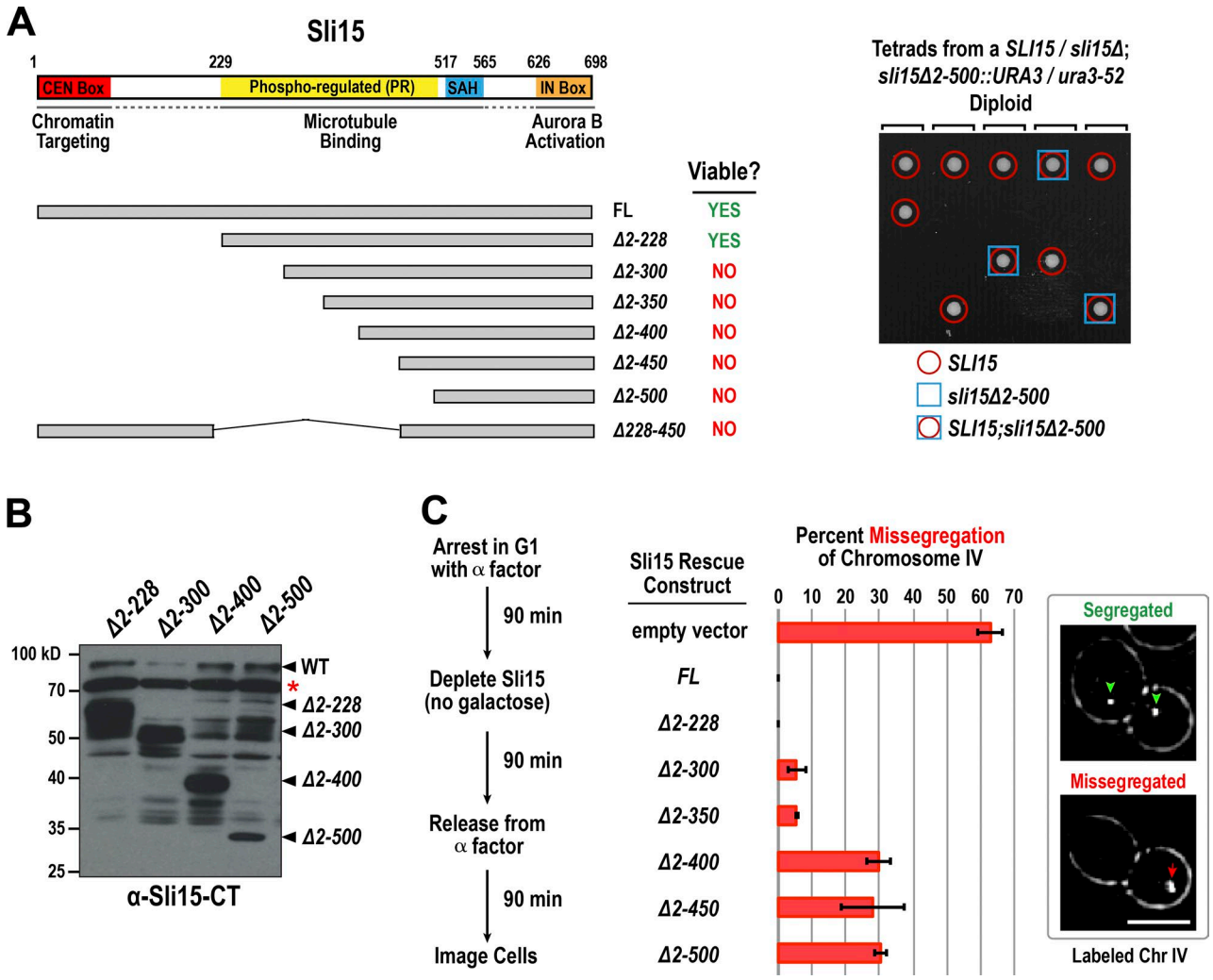

Figure 1. **The PR region of Sli15's microtubule-binding domain is essential for viability and contributes to chromosome segregation fidelity.** (A) Phenotype of Sli15 truncation mutants as assayed by tetrad dissection of diploids heterozygous for *SLI15* at the native locus and the truncation mutant at the *URA3* locus. An example of one tested truncation that is unable to support viability is shown on the right. Note that seven spores that should have had only *sli15Δ2–500* failed to produce colonies. (B) Immunoblots of extracts from the indicated Sli15 truncation mutant strains with an antibody raised to the C terminus (CT) of Sli15. The asterisk indicates a nonspecific band recognized by the primary antibody, which served as a loading control. (C) Analysis of segregation fidelity of GFP-labeled chromosome IV for different Sli15 truncation mutants in the first cell division after depletion of full-length (FL) Sli15 using the protocol described on the left. Images on the right show examples of properly segregated (green arrowheads) and missegregated (red arrow) chromosome IV. The mean percent missegregation observed in three experiments is plotted. Error bars represent SD. At least 100 total cells were counted over the three independent experiments. Bar, 5 µm.

that Sli15 is not dimeric in vivo (Fig. S1 A), similar to what has been shown for INCENP in human cells (Klein et al., 2006).

To confirm that the PR region contributes to microtubule localization in vivo, we generated Venus fusions of GST-dimerized truncations and imaged them in asynchronous cells or cells arrested in metaphase by Cdc20 depletion (Figs. 2 E and S1 B). As shown previously (Campbell and Desai, 2013), deletion of the CEN box caused an increase in CPC localization to the metaphase spindle (Figs. 2 E and S1 B), potentially because of a decreased phosphorylation of the PR region. Consistent with this, progressive deletions of the PR region reduced the elevated localization on the metaphase spindle. The decrease in spindle localization upon PR region deletion was not caused by differences in protein expression; however, the decrease in spindle localization for full-length Sli15 upon the addition of GST likely was caused by decreased expression (Fig. S1 C). For mutants with the largest deletions, GST-Sli15Δ2–450 and GST-Sli15Δ2–500, preanaphase spindle fluorescence was not abolished but was similar to full-length Sli15 (Fig. S1 B). Thus, the deletions of the PR region that are lethal unless rescued by dimerization contribute to preanaphase spindle association in vivo.

We conclude that artificial dimerization mediated by two different means rescues the lethality and substantial chromosome missegregation observed after deletion of the PR region of the Sli15 microtubule-binding domain.

Artificial dimerization does not suppress the lethality of the Sli15 microtubule-binding domain deletions by promoting global Ipl1 kinase activation

We next wanted to test the model that dimerization rescued deletions within the microtubule-binding domain by promoting transphosphorylation-based kinase activation (Fig. 3 A). For

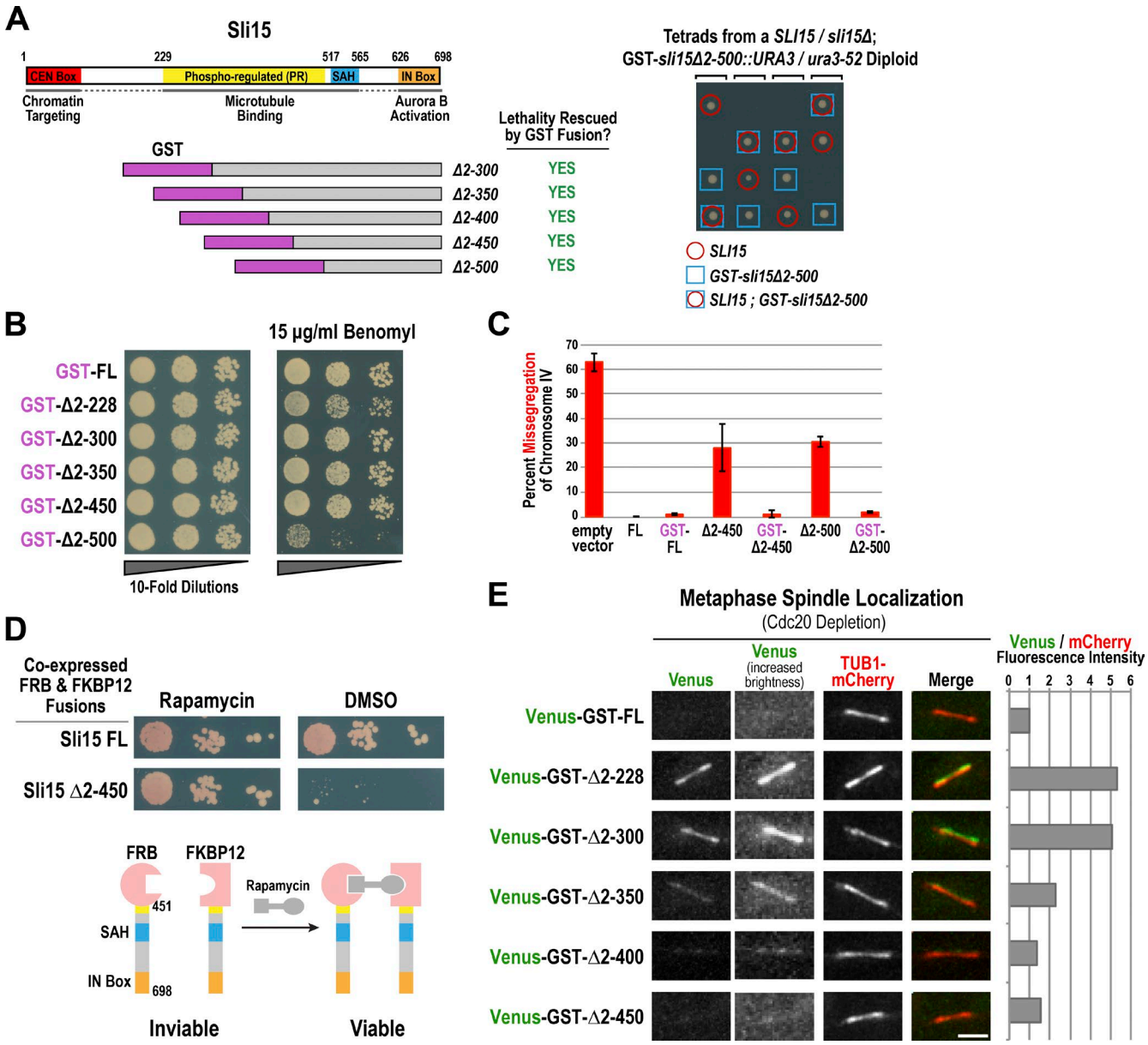

Figure 2. **Artificial dimerization of Sli15 rescues deletion of the PR region of its microtubule-binding domain.** (A) Phenotype of Sli15 truncation mutants with GST conjugated to the N terminus as assayed by tetrad dissection of diploids heterozygous for *SLI15* at the native locus and the GST-fused truncation mutant at the *URA3* locus. The example tetrad dissection on the right shows that all four spores expressing only GST-Sli15Δ2–500 formed colonies. (B) 10-fold serial dilution analysis of growth in the absence (left) or presence (right) of the microtubule-depolymerizing drug benomyl of the indicated Sli15 mutants. (C) Analysis of segregation fidelity of GFP-labeled chromosome IV, conducted as in Fig. 1 C. The mean percent missegregation observed in three experiments is plotted. Error bars represent SD. At least 100 total cells were counted over the three independent experiments. (D) Serial dilution analysis of cells coexpressing the indicated FRB and FKBP12 fusions of Sli15. Culture dilutions were spotted on plates with either 100 μg/ml Rapamycin to induce dimerization or DMSO as a solvent control. The schematic below depicts the experimental design and result. (E) Images of spindles from cells expressing Tub1-mCherry (microtubules) and Venus-GST Sli15 truncation mutants arrested in metaphase by depletion of Cdc20. Images with the same fluorophore were contrast adjusted equally. Spindle intensities were measured by drawing line scans perpendicular to the spindle axis, fitting the intensity values along the line scan to a Gaussian curve, and integrating the area under the curve that was above background. Shown is the mean of 20 spindles quantified for each strain. See Fig. S1 B for similar analysis of unsynchronized cells. Bar, 2 μm. Chr, chromosome; FL, full-length.

this purpose, we used the chemically inducible dimerization system to engineer heterodimers of Sli15Δ2–450, in which one of the two copies of Sli15 harbored two mutations in the IN box (W646G and F680A; Fig. 3 B). W646 and F680 are ubiquitously conserved IN box residues that contact two locations on the Aurora B kinase N-lobe surface and contribute significant binding affinity (Sessa et al., 2005). Consistent with their conservation and importance for kinase binding, full-length Sli15 with W646G and F680A mutations failed to rescue viability after depletion of endogenous Sli15 (Fig. S2 A).

Rapamycin-induced heterodimers engineered to bind only one copy of Ipl1 rescued the Δ2–450 PR region deletion (Fig. 3 C), demonstrating that transphosphorylation-based activation is not critical for the phenotypic suppression observed after inducible dimerization. This rescue required the presence of both the FRB and FKBP12 constructs (Fig. S2

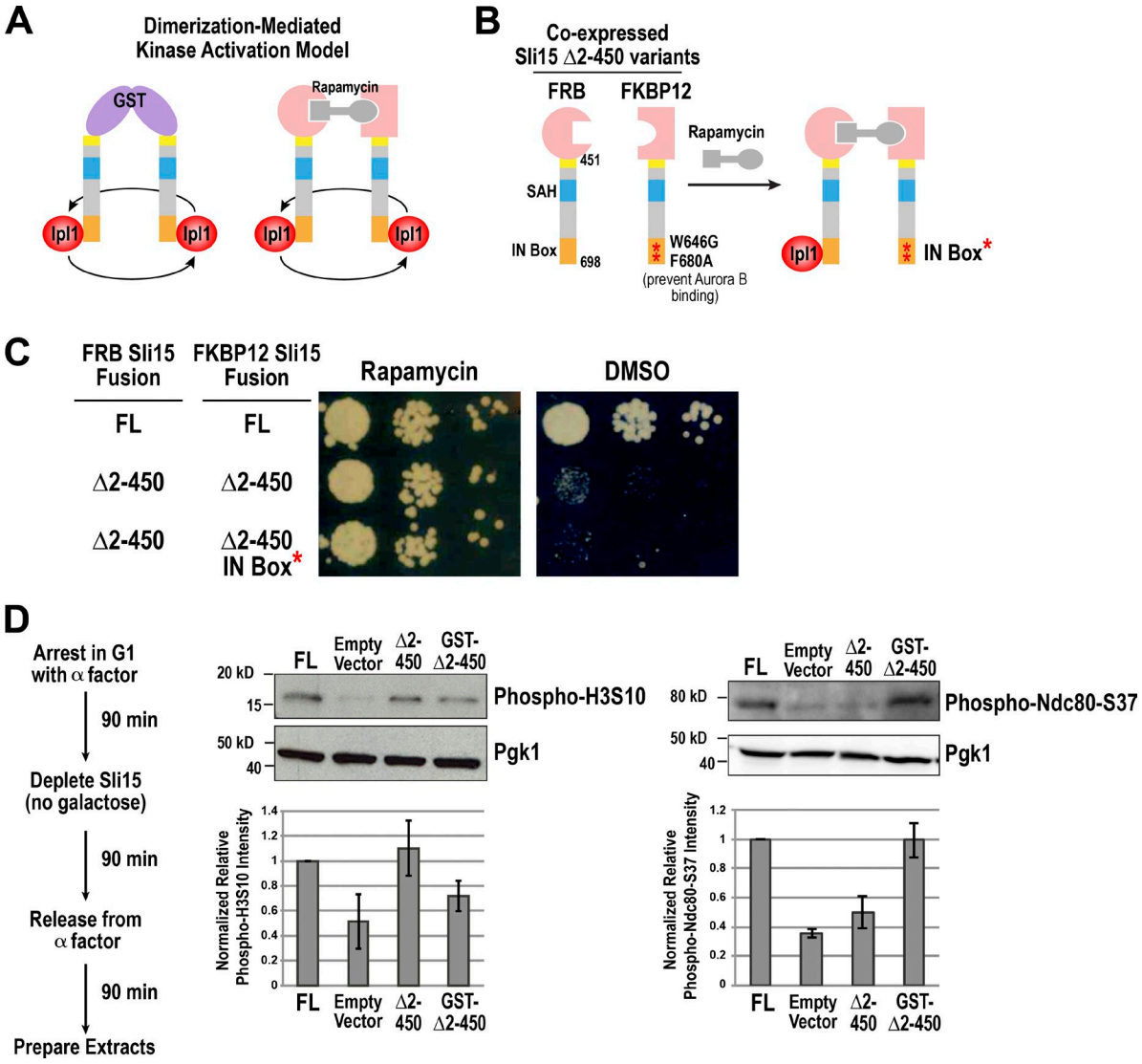

Figure 3. **Artificial dimerization does not rescue viability of Sli15 truncations by globally increasing Ipl1 kinase activation.** (A) Schematic of a model based on prior work in which dimerization enhances kinase activation by bringing two kinase subunits in physical proximity and promoting transphosphorylation. (B) Schematic of experiment designed to test the dimerization-induced kinase activation model. IN box* denotes two point mutations that decrease Ipl1 binding. (C) Results of the controlled dimerization-based test of the kinase activation model. The coexpressed fusions are indicated on the left, and culture dilutions spotted on plates with Rapamycin or DMSO are shown on the right. (D) Immunoblotting analysis of histone H3 phosphorylation on serine 10 and Ndc80 phosphorylation on serine 37 from the indicated Sli15 variant–expressing strains after depletion of full-length (FL) Sli15. Phosphoglycerate kinase 1 (Pgk1) served as a loading control. The means of three experiments are shown below each blot. Error bars represent SEM.

B), suggesting that dimerization rescues deletion of the PR region through a mechanism that is independent of clustering-based kinase activation.

To confirm the aforementioned result using an independent assay, we measured phosphorylation of the conserved Aurora B substrate histone H3 on serine 10. H3S10 phosphorylation is ubiquitous throughout mitosis irrespective of the attachment state of the kinetochores and serves as a readout for global kinase activity. Depletion of full-length Sli15 using a promoter shutoff decreased H3S10 phosphorylation (Fig. 3 D). In contrast, Sli15Δ2–450 exhibited H3S10 phosphorylation equal to that of full-length Sli15 (Fig. 3 D), and fusion of this fragment to GST did not elevate H3S10 phosphorylation but instead appeared to modestly decrease it. In addition, chromosome missegregation or spindle checkpoint–mediated arrest phenotypes associated with increased Ipl1 kinase activity after overexpression (Muñoz-Barrera and Monje-Casas, 2014) were not observed after dimerization (not depicted).

To address the effect of Sli15 truncations on the phosphorylation of kinetochore substrates of Ipl1, we used an antibody raised against a peptide containing phosphorylated serine 37 of the kinetochore protein Ndc80. Immunoblots revealed a similar decrease in signal after the depletion of Sli15 (Fig. 3 D) or in a temperature-sensitive Ipl1 mutant (Fig. S2 C). No signal was detected when seven Ipl1 consensus sites in Ndc80, including serine 37, were mutated to alanine (Akiyoshi et al., 2009), confirming the phosphospecificity of the antibody (Fig. S2 C). In contrast to H3S10 phosphorylation, Ndc80 serine 37 phosphorylation was not restored by the Sli15Δ2–450 mutant but was restored by fusion of GST to Sli15Δ2–450. Thus, deletion of the majority of the PR region does not affect global kinase activity, but it reduces the phosphorylation of a kinetochore substrate,

and consistent with the rescue of chromosome segregation and viability, fusion of the truncated Sli15 to GST restores kinetochore substrate phosphorylation.

Collectively, these results indicate that dimerization of the Sli15 microtubule-binding domain deletion mutants does not act by promoting global kinase activation but restores targeting of kinetochore substrates, which is likely the basis for the rescue of viability.

Artificial dimerization promotes spindle microtubule localization

As the largest GST-fused PR region deletions exhibited microtubule localization similar to full-length Sli15 during anaphase (Fig. S1 B), we next wanted to test whether artificial dimerization acted by promoting microtubule localization. For this purpose, we added the mNeonGreen fluorophore to the C terminus of FKBP12-Sli15Δ2–450 and compared the effects of removing or adding back Rapamycin on localization (Fig. 4 A). In the presence of Rapamycin and FRB-Sli15Δ2–450, we observed robust mNeonGreen signal at both anaphase and preanaphase spindles (the signal was stronger with the mNeonGreen fusion relative to the Venus fusions likely because of its superior fluorophore properties in vivo; Fig. 4 B). Spindle localization decreased significantly when cells were switched to media without Rapamycin (Fig. 4, B and C). When Rapamycin was returned to the media, mNeonGreen signal rapidly and fully returned to the spindles (Fig. 4, B and C). Expression of the mNeonGreen-conjugated fusion was not altered by the presence or absence of Rapamycin (Fig. 4 D). These data indicate that induced dimerization increases the spindle association properties of either the C-terminal part of Sli15 or of Ipl1 that is bound to the Sli15 IN box. Furthermore, the results suggest a correlation between spindle association (Fig. 4, B and C) and the ability to promote chromosome biorientation and support viability (Fig. 2 D).

Spindle localization observed after artificial dimerization of Sli15 truncations requires the putative SAH of Sli15

The aforementioned results suggest that dimerization promotes microtubule association of a region distal to amino acid 500 of Sli15 or of Ipl1 bound to Sli15. The SAH of INCENP, incorrectly predicted as a coiled-coil that ends ∼50 amino acids before the IN box in vertebrates, is required for enrichment of the CPC on anaphase spindles in human cancer cell lines and binds directly to microtubules (Samejima et al., 2015; van der Horst et al., 2015), making it a good candidate for a microtubule-binding domain whose affinity is promoted by dimerization. In Sli15, which is not dimeric (Fig. S1 A), coiled-coil predictions identify residues 520–565, and we therefore refer to these residues as the SAH (Fig. 5 A). Similar to the results with Rapamycin-induced dimerization, addition of GST to a Venus-tagged Sli15 construct that lacks the N-terminal 500 amino acids increased the localization to the spindle in the first cell division after depletion of full-length Sli15 (Fig. 5 B). To determine whether the SAH is required for this spindle localization, we deleted an additional 74 amino acids that include the putative SAH domain. Venus–GST-Sli15Δ2–574 exhibited strongly decreased spindle association both before and after anaphase onset (Fig. 5 B). Thus, artificial dimerization of a Sli15 fragment lacking the first 500 amino acids promotes spindle association, and this association requires the SAH that immediately follows the truncated region.

The putative SAH of Sli15 is essential for chromosome biorientation and viability

As the SAH of Sli15 is required for spindle localization, we next determined its contribution to chromosome segregation and viability. Spores containing deletions of Sli15 that remove the SAH alone or together with the CEN box and the PR region failed to form colonies, even when fused to GST, indicating that the SAH is essential for viability, is not interchangeable with the PR region, and cannot be compensated for by artificial dimerization (Figs. 6 A and S3, A and B). Consistent with this, Rapamycin-induced dimerization of Sli15 missing only the SAH (*Δ520–574*) also failed to rescue viability (Fig. 6 B). A heterodimer consisting of one Sli15 molecule missing the SAH and another Sli15 with point mutants in the IN box was also inviable, suggesting that the SAH and the IN box cannot act in trans (Fig. 6 B). Furthermore, the chromosome missegregation rate of a GST-fused mutant that deletes both the PR and SAH regions (GST-*Δ2*–574) was comparable with Sli15 depletion (Fig. 6 C; compare with Fig. 2 C).

To determine whether removal of the SAH leads to a penetrant Sli15 loss-of-function phenotype because it is required to activate Ipl1 in vivo, we analyzed H3S10 phosphorylation, which is significantly reduced by Sli15 depletion (Figs. 3 D and 6 D). The GST-Δ2–574 mutant exhibited H3S10 phosphorylation close to wild-type levels (Fig. 6 D), indicating that the extreme C-terminal 124 amino acids of Sli15, which include the IN box, are sufficient for kinase activation. In contrast to H3S10, phosphorylation of the kinetochore substrate Ndc80 at serine 37 was reduced in the GST-Δ2–574 mutant to a comparable level as Sli15 depletion (Fig. 6 D). We confirmed a reduced phosphorylation of kinetochore substrates in this mutant by analyzing the electrophoretic mobility of Dam1, a subunit of the kinetochore-localized microtubule-binding Dam1 complex that is targeted by Ipl1. A shift in Dam1 mobility is detectable that is sensitive to phosphatase treatment, to temperature-sensitive inactivation of Ipl1, and to depletion of Sli15 (Figs. 6 D and S3 C; Storchová et al., 2011; Muñoz-Barrera and Monje-Casas, 2014). In the GST-Sli15Δ2–574 mutant, the shift in Dam1 mobility was reduced to the same degree as Sli15 depletion (Fig. 6 D). Thus, phosphorylation of two major Ipl1 targets at the kinetochore, Ndc80 and Dam1, requires the SAH of Sli15, irrespective of artificial dimerization. We conclude that the putative SAH of Sli15 is dispensable for the global activation of Ipl1 but is required for the kinase activity to target substrates at the kinetochore, and this requirement cannot be superseded by artificial dimerization.

Discussion

In budding yeast, the Aurora kinase Ipl1 promotes biorientation by correcting the naturally high frequency of syntelic attachments that are caused by centromere replication and kinetochore formation before maturation of the daughter spindle pole body (Tanaka et al., 2002). As in other species, Ipl1 is present in a complex with the conserved CPC subunits Sli15/INCENP, Bir1/Survivin, and Nbl1/Borealin. In this study, we define a minimal biorientation module that is sufficient for viability and contains only the C-terminal region of Sli15/INCENP together with Ipl1 (Fig. 7 A). The engineered Sli15 in this module lacks ∼70% of its primary amino acid sequence, including the centromere/chromatin localization domain that is required to bind to Bir1/

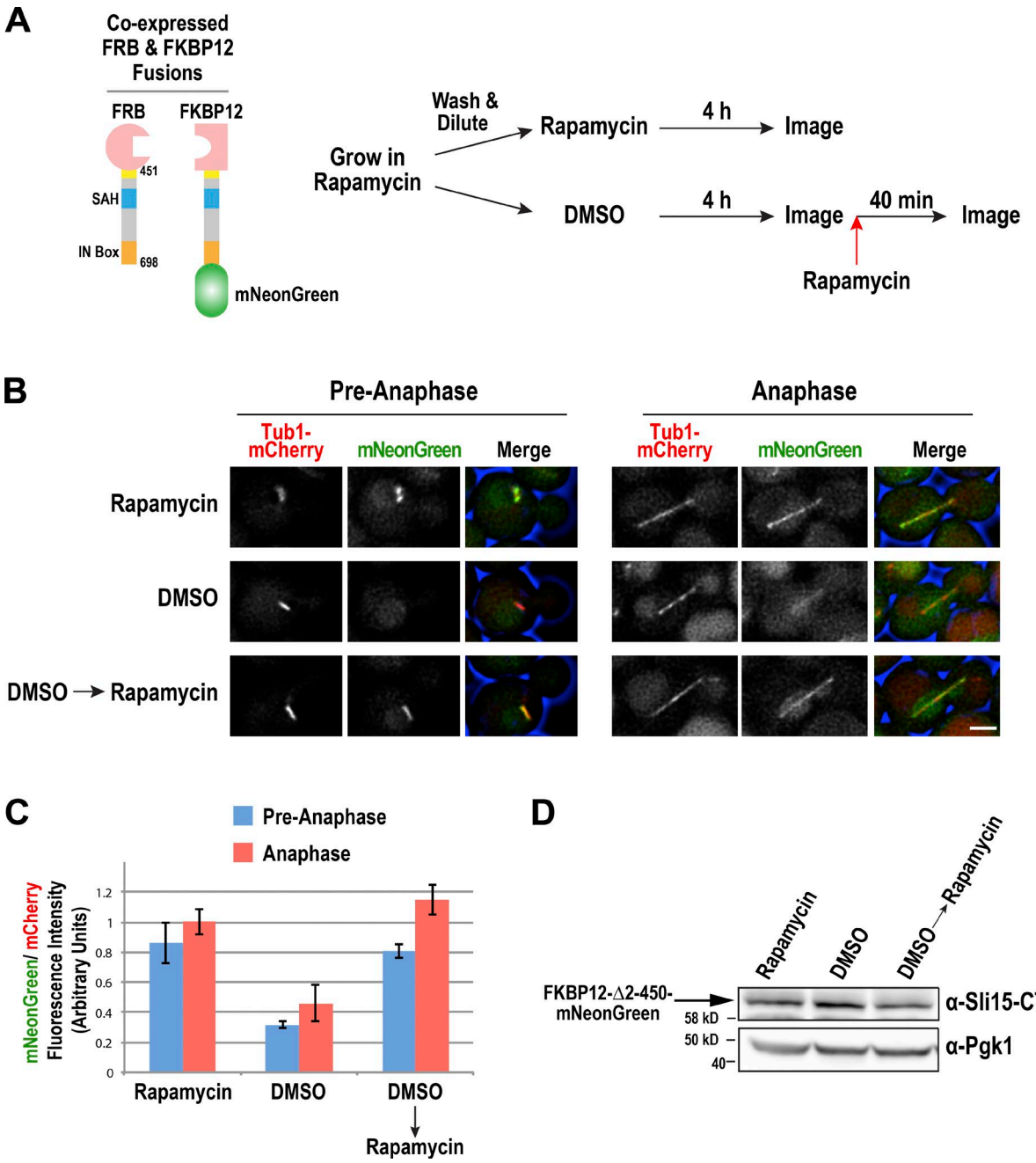

Figure 4. **Artificial dimerization of Sli15Δ2–450 enhances its localization to the mitotic spindle.** (A) Schematic of the expressed Sli15Δ2–450 fusions (left) and the experimental protocol used to analyze the effects of dimerization on spindle localization (right). (B) Example images of preanaphase (left) and anaphase (right) spindles in the three indicated conditions. In the Merge panels, cell outlines are shown in blue. Bar, 2 µm. (C) Spindle intensities quantified as in Fig. 2 E for the indicated conditions. The mean of three independent experiments is shown. Error bars represent SEM. (D) Immunoblots of extracts from samples treated as shown in A with an antibody that recognizes the C terminus of Sli15. Phosphoglycerate kinase 1 (Pgk1) served as a loading control.

Survivin-Nbl1/Borealin in vivo (Campbell and Desai, 2013) as well as a large segment of its central region that contributes to spindle association and is phosphorylated by Cdk1 and Ipl1.

This minimal CPC is only functional in combination with induced dimerization (Fig. 7 A). Although we and others have been unable to identify an oligomeric form of INCENP in vivo (Fig. S1 A; Klein et al., 2006), there is evidence from human cell culture that Borealin dimerization contributes to the spindle checkpoint function of the CPC (Bekier et al., 2015). Notably, dimerization-based rescue of lethality by the minimal CPC is not caused by the promotion of transphosphorylation-based activation of the kinase, a prominent model for how dimerization/clustering influences CPC function (Kelly et al., 2007; Tseng et al., 2010). Instead, artificial dimerization promotes localization to the spindle and restores the phosphorylation of kinetochore substrates, suggesting that preanaphase spindle association is important for Ipl1 to execute its biorientation function.

Deletions within the microtubule-binding domain of Sli15 severely disrupt the chromosome segregation function of the CPC and are lethal. This is in contrast to mutants that prevent or mimic phosphorylation in this region, which display little to no growth defects (Pereira and Schiebel, 2003; Nakajima et al.,

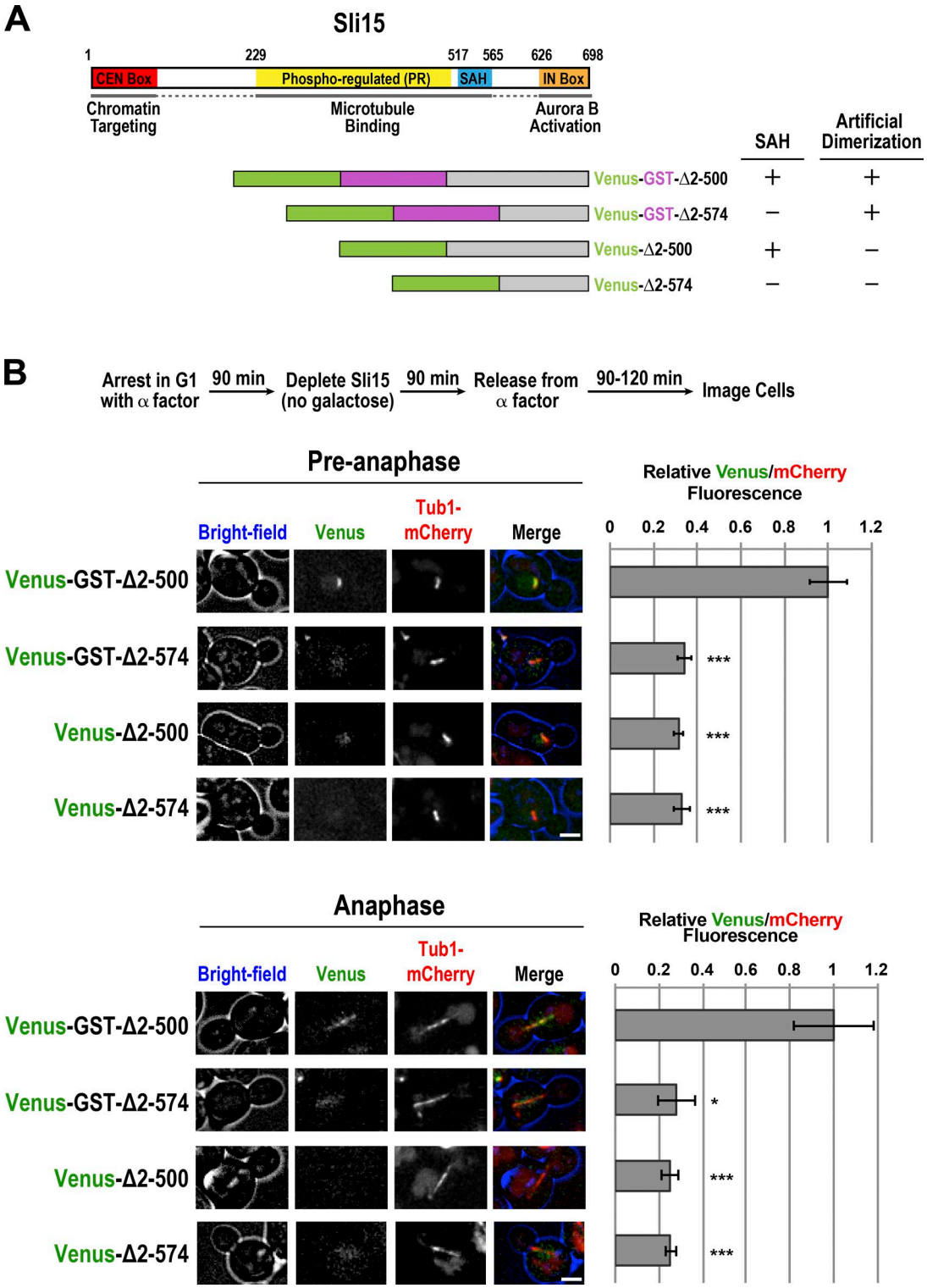

Figure 5. **The SAH of Sli15 is required for spindle association after artificial dimerization.** (A) Schematic of Sli15 truncations engineered to test the role of the SAH in Sli15 localization with and without GST-mediated dimerization. (B) Images of spindles from cells expressing Tub1-mCherry (microtubules) and Venus-conjugated Sli15 truncation mutants. Images with the same fluorophore were contrast adjusted equally. Spindle intensities were measured by drawing line scans perpendicular to the spindle axis, fitting the intensity values along the line scan to a Gaussian curve, and integrating the area under the curve that is above background. The Venus-Sli15 integrated signal was divided by the mCherry-Tub1 signal for each spindle. The means and SEM are plotted. *, $P < 0.05$; ***, 0.0001; unpaired *t* test in comparison with Venus-GST-Δ2–500 at the indicated stage of mitosis. From the top, the numbers of cells quantified for each construct are 39, 45, 61, 52, 16, 6, 32, and 20. Bars, 2 µm.

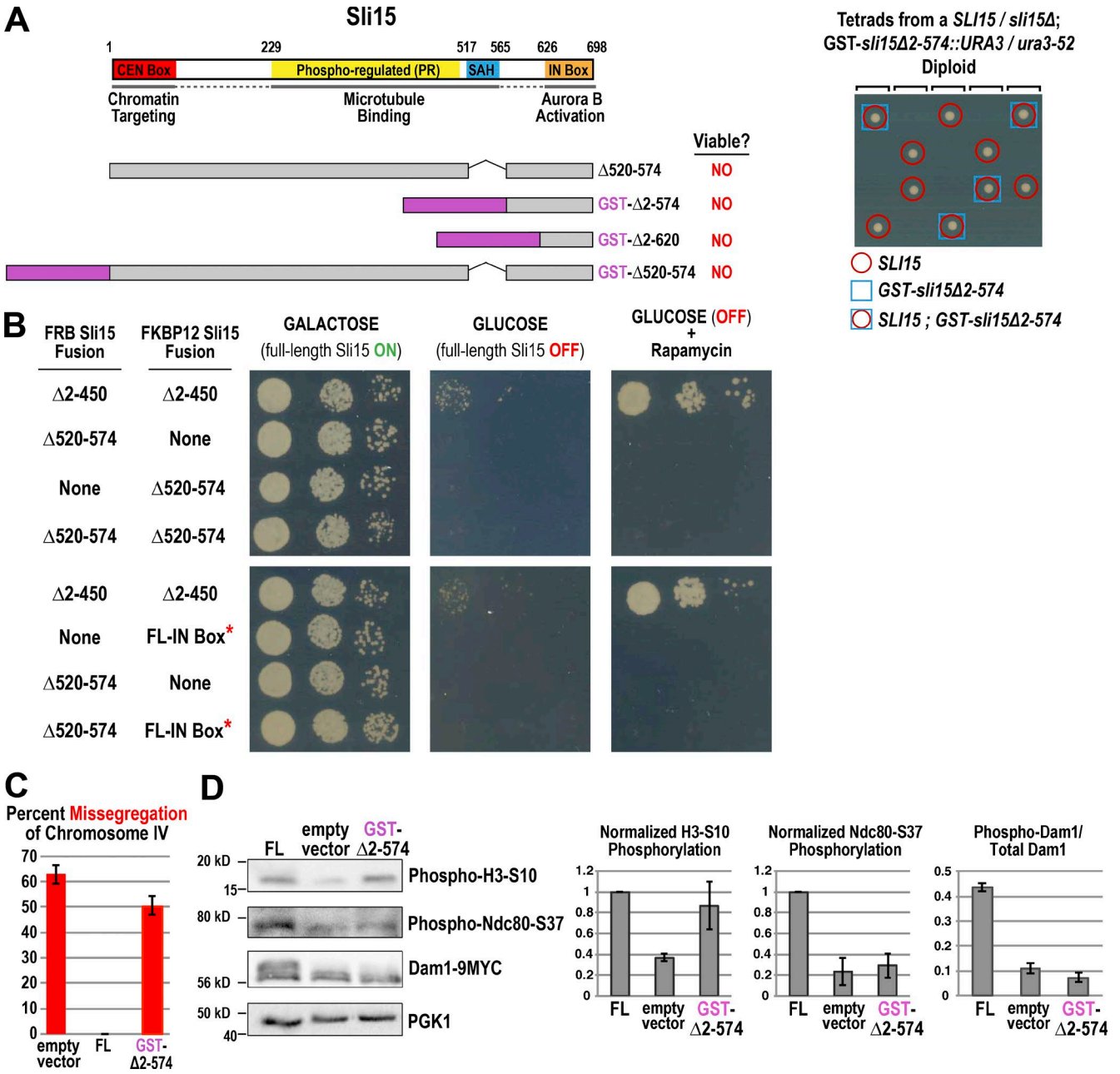

Figure 6. **The Sli15 SAH domain is essential for chromosome segregation and kinetochore phosphorylation.** (A) Phenotype of Sli15 SAH truncation mutants as assayed by tetrad dissection of diploids heterozygous for *SLI15* at the native locus and the truncation mutant at the *URA3* locus. An example of one tested truncation that is unable to support viability is shown on the right. Note that six spores that should have had *GST-sli15Δ2–574* as the sole copy of the *SLI15* gene failed to produce colonies. (B) Serial dilution analysis of cells with the indicated Sli15 variants and another copy of Sli15 under the control of a galactose-inducible promoter. Diluted cultures were spotted on the indicated plates. 100 µg/ml Rapamycin was used to induce dimerization. IN box* denotes two point mutations that decrease Ipl1 binding. (C) Analysis of segregation fidelity of GFP-labeled chromosome IV, conducted as in Fig. 1 C. The mean percent missegregation observed in three experiments is plotted. Error bars represent SD. At least 100 total cells were counted for each mutant. (D) Immunoblots of extracts from the indicated Sli15 variants expressing strains after depletion of full-length (FL) Sli15. Membranes were probed with antibodies that recognize histone H3 phosphorylated on serine 10, a 9-MYC tag inserted at the C terminus of endogenous Dam1, and Ndc80 phosphorylated on serine 37. Phosphoglycerate kinase 1 (Pgk1) served as a loading control. The means of three experiments are shown. Error bars represent SEM.

2011; Makrantoni et al., 2014). Based on this difference, we suggest that phosphorylation of this region of Sli15 allows for weak spindle association, which is enhanced upon dephosphorylation in anaphase. Localization of the CPC to preanaphase spindles has been previously reported in budding yeast (Buvelot et al., 2003; Nerusheva et al., 2014), *Xenopus laevis* egg extracts (Tseng et al., 2010), and HeLa cells (Banerjee et al., 2014). Our emphasis on the importance of this preanaphase spindle association in biorientation comes from the key features of the minimal biorientation module: the putative SAH, the kinase-binding IN box, and the catalytic Ipl1 kinase subunit. The IN box and Ipl1 are both essential for kinase activity; in contrast, the SAH is not required for global kinase activation but is required to target kinetochore substrates. Based on the correlation between dimerization-based rescue and spindle association, we propose that the SAH by itself has low affinity for microtubules,

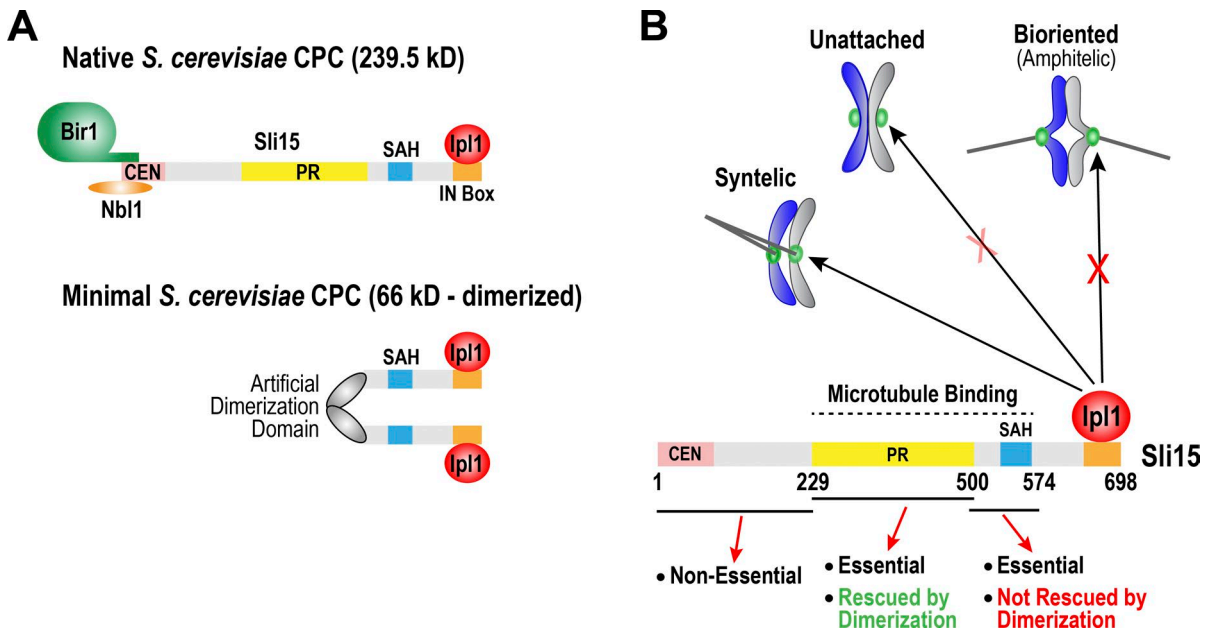

Figure 7. **Schematic summary of key results.** (A) Diagram of the native *S. cerevisiae* CPC compared with the functional minimal CPC engineered in this study. The minimal CPC contains the putative SAH domain, the Ipl1-binding IN box, and an artificial dimerization domain. The Bir1 and Nbl1 subunits as well as the CEN and PR domains are dispensable for the essential chromosome biorientation function of the CPC. (B) Schematic of results for deletions of different regions of the Sli15 microtubule-binding domain. Deletion of the PR region is lethal but can be rescued via artificial dimerization. Deletion of the SAH region is essential and cannot be rescued. These results suggest a role for microtubule binding of Sli15 in sensing improper attachment states for chromosomes during alignment. One possible role for microtubule binding is to increase CPC activity at kinetochores on syntelic versus unattached chromosomes, as only syntelic attachments require correction by the CPC. An additional property, such as tension, would be used to prevent CPC activity at the kinetochores of bioriented chromosomes.

but the PR domain, via its independent weak affinity, generates sufficient preanaphase microtubule-associated, IN box–bound, and activated Ipl1 to correct syntelic attachments (Fig. 7 B). This model suggests why removal of the PR region can be compensated for by artificial dimerization, as it brings together two SAHs, and the consequent increased avidity enhances microtubule binding. This proposal is supported by the ability of the SAH from INCENP to directly bind microtubules (Samejima et al., 2015; van der Horst et al., 2015) and by the negative effect of SAH deletion on INCENP localization to microtubules (van der Horst et al., 2015). Additionally, an INCENP mutant lacking the SAH fails to activate the spindle checkpoint in response to taxol treatment in human U2OS cells (Vader et al., 2007). One potential reason for why microtubule association is important is that it may lead to a reduction in dimensionality, increasing the activity of Aurora B toward microtubule-bound substrates (Noujaim et al., 2014). Microtubule association may also help preferentially target incorrectly microtubule-bound versus unattached kinetochores (Fig. 7 B). This view is in agreement with analysis in human cells that showed a graded degree of Ndc80 phosphorylation with kinetochores in prometaphase cells exhibiting the highest phosphorylation, followed by unattached kinetochores in nocodazole-treated cells, and finally kinetochores of metaphase cells (DeLuca et al., 2011).

In contrast to the PR region, truncations removing the SAH of Sli15 cannot be compensated for by dimerization. Thus, the PR region and the SAH are not interchangeable, and the SAH is essential for biorientation regardless of dimerization (Fig. 7 B). In preliminary work, lethality caused by point mutants that decrease the spindle localization of Sli15's SAH is suppressed by mutations that increase the spindle binding of the PR domain, supporting the notion that the SAH contributes to chromosome biorientation at least in part through spindle association (unpublished data). The fact that the SAH has specific physical characteristics suggests that microtubule association may not be its only activity relevant for biorientation. Our attempts to replace the SAH with microtubule-binding regions from three different yeast microtubule-associated proteins have not been successful to date (Stu2, Irc15, and She1; unpublished data), which indicates that the SAH may serve an additional function. This view is supported by the inability of the SAH to function with the IN box in trans, suggesting that the two domains need to be adjacent on the same polypeptide. The special property of the SAH could be a particular mode of microtubule binding, tethering of the activated kinase at a specific distance from the microtubule surface based on its predicted extended structure, or an additional, as yet unidentified, function, such as mediating binding to a site at the kinetochore. Our definition of a minimal module that provides the essential biorientation function of the CPC in budding yeast should help address the fascinating and challenging question of how cells detect and correct errors in chromosome–spindle attachments to ensure accurate segregation of the genome.

Materials and methods

Yeast strains and media

See Table S1 for all yeast strains and plasmids used in this study. Strains were grown in either yeast extract/peptone supplemented with 40 µg/ml adenine-HCl (YPA) or synthetic media with 2% sugars. Rapamycin (Santa Cruz Biotechnology, Inc.) was used at a concentration of 100 ng/ml. Cultures were incubated at 30°C unless otherwise indicated. Epitope and fluorescent tags were inserted at the C terminus of genes at

their native loci as described previously (Longtine et al., 1998). Gene truncations and point mutants of plasmids were made using Gibson assembly (Gibson et al., 2009). PCR products were purified from agarose gels and combined 1:1 with Assembly Master Mix (1 U/µl T5 exonuclease, 33 U/ml Phusion DNA polymerase, 5 U/µl Taq DNA ligase, 13 mM magnesium chloride, 13 mM dithiothreitol, 8 µM deoxynucleotides, 1.3 mM nicotinamide adenine dinucleotide [NAD^+; New England Biolabs, Inc.], 67 mg/ml polyethylene glycol, and 133 mM Tris, pH 7.5), incubated for 1 h at 50°C, and transformed into chemically competent bacteria. Plasmids were integrated either at their native loci or at the URA3 or HIS3 loci by digesting the plasmids with the StuI, EcoRV, or SnaBI restriction enzymes. All plasmids and integrations were checked by PCR and sequencing.

Immunoprecipitation and Western blotting

To immunoprecipitate Sli15-6HA, 50 ml cells in exponential growth were pelleted and resuspended in 600 µl immunoprecipitation buffer with protease inhibitors (50 mM Tris, pH 7.6, 150 mM NaCl, 1% Triton X-100, 1 mM EDTA, 2 mM phenylmethylsulphonyl fluoride, 4 mM benzamidine, and cOmplete EDTA-free protease inhibitor cocktail [Roche]) and vortexed for 45 min with 400 µl glass beads at 4°C. Lysates were cleared at 18,000 *g* for 10 min, transferred to a new tube, and centrifuged again. A total of 25 µl of antibody–bead slurry (anti-HA monoclonal clone 3F10; Roche) was combined with 500 µl of cleared lysate and rotated at 4°C for 1 h. Beads were washed once with immunoprecipitation buffer and three times with Tris-buffered saline, pH 7.4, and then were resuspended in 100 µl protein sample buffer. Whole-cell extracts were prepared for Western blotting by pelleting 2 ml of cultures in exponential growth and resuspending them in 100 µl sample buffer and 30 µl glass beads. Samples were then vortexed at 4°C for 30 min and centrifuged at 18,000 *g* for 5 min. Extracts for phosphoprotein analysis were prepared by pelleting 2 ml of cells, resuspending them in 100 µl of 5% trichloroacetic acid, and incubating them at room temperature for 10 min. The cells were then washed once with water and resuspended in 100 µl lysis buffer (50 mM Tris, pH 7.4, 1 mM EDTA, 50 mM DTT, cOmplete EDTA-free protease inhibitor cocktail, and PhosSTOP [Roche]) plus glass beads. Samples were vortexed at 4°C for 30 min, followed by addition of 33 µl of 4× sample buffer.

For immunoblots, samples were separated on 10% or 15% acrylamide gels, transferred to nitrocellulose membranes, and blotted with one of the following antibodies: Sli15–rabbit polyclonal raised against the C terminus (Sandall et al., 2006), HA–clone 3F10 (Roche), Myc–mouse monoclonal 4A6 (EMD Millipore), H3–rabbit polyclonal 9715 (Cell Signaling Technology), Phospho-H3S10–rabbit polyclonal D2C8 (Cell Signaling Technology), Pgk1–mouse monoclonal 22C5D8 (Thermo Fisher Scientific), and Ndc80 phospho-S37–rabbit polyclonal (a gift from S. Biggins, Fred Hutchinson Cancer Research Center, Seattle, Washington). The Ndc80 antibody was incubated with unphosphorylated competitor peptide at 5× concentration by mass. The membranes were then probed with horseradish peroxidase–conjugated secondary antibodies. Intensities of the blots were quantified using ImageJ (National Institutes of Health).

Microscopy

Overnight cultures were diluted 100-fold and grown out of stationary phase for 4–5 h. Cells were pelleted by brief centrifugation, washed once and resuspended in water, placed on 1% agarose pads supplemented with complete synthetic media, covered with a coverslip, and sealed around the edges with VALAP (a 1:1:1 mixture of petroleum jelly [Vaseline], lanolin, and paraffin [Thermo Fisher Scientific] by weight). Images were collected on a DeltaVision microscopy system (Applied Precision, Ltd.) at 22°C using a 60×, 1.35 NA Olympus U-Plan Apochromat objective and a CoolSNAP charge-coupled device camera (Photometrics). 14 z-sections were taken with 0.5-µm steps and deconvolved with softWoRx software (Life Sciences Software). Further image analyses, including maximum-intensity projections and contrast adjustments, were performed in ImageJ. Images within each figure were all collected on the same day and contrast adjusted identically. Spindles were determined to be preanaphase if they were >2 µm in length and had not yet aligned with the bud neck. Anaphase spindles were categorized as those that had passed through the bud neck but had not yet reached the ends of the mother/bud. Spindles of similar length were used for quantification. Quantification of spindle intensities was performed by first taking a line scan in ImageJ perpendicular to the spindle with a 5-pixel-wide line. The intensity profile was then analyzed using a custom python script that fits a Gaussian curve to the line scan and calculates the area under the Gaussian fit (Text S1).

For chromosome segregation assays, Sli15 expressed from the *Gal10-1* promoter was depleted by first synchronizing cells for 90 min in YPA plus 1% galactose and 1% raffinose (YPAGR) and 10 µM α-factor. The cultures were then switched to YPA plus 2% glucose (YPAD) and 10 µM α-factor for 90 min to deplete Sli15. To release from G1 arrest, cells were washed five times with fresh YPAD and incubated for an additional 90 min before imaging. For metaphase arrest with Cdc20 depletions, asynchronous cultures in YPAGR were washed three times and switched to YPAD media for 2.5 h before imaging.

Tetrad dissection

Diploid strains were sporulated by first growing them on YPAD plates overnight at 30°C and then transferring them to sporulation plates (8.2 mg/ml sodium acetate and 16 mg/ml agar) and incubating at 23°C for 2–3 d. Spores were then washed with water and digested with 1 mg/ml zymolyase (Zymo Research) for 5–10 min at 30°C and then dissected onto YPAD or YPAD plus Rapamycin plates. Genotyping was performed by replica plating onto selective media.

Online supplemental material

Fig. S1 shows additional experiments and controls to accompany Fig. 2, including an immunoprecipitation experiment with two differently labeled forms of Sli15, localization of Sli15 variants at different cell cycle stages, and quantification of Sli15 mutant expression by Western blotting. Fig. S2 contains controls for experiments in Fig. 3. Fig. S3 shows controls and example images for experiments in Fig. 6. Table S1 contains a list of all of the yeast strains and plasmids used in this study and includes the figures in which the corresponding strains were used. Text S1 shows code for a python script used to measure fluorescence intensity on the mitotic spindle.

Acknowledgments

The authors thank the Desai, Oegema, and Campbell laboratories for helpful discussions and for comments on the manuscript. We thank Sue Biggins for the gifts of yeast strains, peptides, and the Ndc80 phosphoantibody.

This work was supported by National Institutes of Health grant GM074215 to A. Desai and Vienna Science and Technology Fund grant VRG14-001 and Austrian Science Fund grant Y 944-B28 to C.S. Campbell. A. Desai receives salary and other support from the Ludwig Institute for Cancer Research.

The authors declare no competing financial interests.

Author contributions: S. Fink performed experiments and edited the manuscript. K. Turnbull performed experiments. A. Desai conceived experiments and edited the manuscript and figures. C.S. Campbell conceived, designed, and performed experiments, wrote the manuscript, and created the figures.

Submitted: 28 September 2016
Revised: 13 January 2017
Accepted: 1 February 2017

References

Akiyoshi, B., C.R. Nelson, J.A. Ranish, and S. Biggins. 2009. Analysis of Ipl1-mediated phosphorylation of the Ndc80 kinetochore protein in *Saccharomyces cerevisiae*. *Genetics.* 183:1591–1595. http://dx.doi.org/10.1534/genetics.109.109041

Banerjee, B., C.A. Kestner, and P.T. Stukenberg. 2014. EB1 enables spindle microtubules to regulate centromeric recruitment of Aurora B. *J. Cell Biol.* 204:947–963. http://dx.doi.org/10.1083/jcb.201307119

Bekier, M.E., T. Mazur, M.S. Rashid, and W.R. Taylor. 2015. Borealin dimerization mediates optimal CPC checkpoint function by enhancing localization to centromeres and kinetochores. *Nat. Commun.* 6:6775. http://dx.doi.org/10.1038/ncomms7775

Biggins, S., and A.W. Murray. 2001. The budding yeast protein kinase Ipl1/Aurora allows the absence of tension to activate the spindle checkpoint. *Genes Dev.* 15:3118–3129. http://dx.doi.org/10.1101/gad.934801

Buvelot, S., S.Y. Tatsutani, D. Vermaak, and S. Biggins. 2003. The budding yeast Ipl1/Aurora protein kinase regulates mitotic spindle disassembly. *J. Cell Biol.* 160:329–339. http://dx.doi.org/10.1083/jcb.200209018

Campbell, C.S., and A. Desai. 2013. Tension sensing by Aurora B kinase is independent of survivin-based centromere localization. *Nature.* 497:118–121. http://dx.doi.org/10.1038/nature12057

Cheeseman, I.M., J.S. Chappie, E.M. Wilson-Kubalek, and A. Desai. 2006. The conserved KMN network constitutes the core microtubule-binding site of the kinetochore. *Cell.* 127:983–997. http://dx.doi.org/10.1016/j.cell.2006.09.039

Cho, U.-S., and S.C. Harrison. 2011. Ndc10 is a platform for inner kinetochore assembly in budding yeast. *Nat. Struct. Mol. Biol.* 19:48–55. http://dx.doi.org/10.1038/nsmb.2178

Cimini, D., X. Wan, C.B. Hirel, and E.D. Salmon. 2006. Aurora kinase promotes turnover of kinetochore microtubules to reduce chromosome segregation errors. *Curr. Biol.* 16:1711–1718. http://dx.doi.org/10.1016/j.cub.2006.07.022

Cooke, C.A., M.M. Heck, and W.C. Earnshaw. 1987. The inner centromere protein (INCENP) antigens: movement from inner centromere to midbody during mitosis. *J. Cell Biol.* 105:2053–2067. http://dx.doi.org/10.1083/jcb.105.5.2053

Dai, J., S. Sultan, S.S. Taylor, and J.M.G. Higgins. 2005. The kinase haspin is required for mitotic histone H3 Thr 3 phosphorylation and normal metaphase chromosome alignment. *Genes Dev.* 19:472–488. http://dx.doi.org/10.1101/gad.1267105

DeLuca, K.F., S.M.A. Lens, and J.G. DeLuca. 2011. Temporal changes in Hec1 phosphorylation control kinetochore-microtubule attachment stability during mitosis. *J. Cell Sci.* 124:622–634. http://dx.doi.org/10.1242/jcs.072629

Gibson, D.G., L. Young, R.-Y. Chuang, J.C. Venter, C.A. Hutchison III, and H.O. Smith. 2009. Enzymatic assembly of DNA molecules up to several hundred kilobases. *Nat. Methods.* 6:343–345. http://dx.doi.org/10.1038/nmeth.1318

Jeyaprakash, A.A., U.R. Klein, D. Lindner, J. Ebert, E.A. Nigg, and E. Conti. 2007. Structure of a Survivin-Borealin-INCENP core complex reveals how chromosomal passengers travel together. *Cell.* 131:271–285. http://dx.doi.org/10.1016/j.cell.2007.07.045

Kalantzaki, M., E. Kitamura, T. Zhang, A. Mino, B. Novák, and T.U. Tanaka. 2015. Kinetochore-microtubule error correction is driven by differentially regulated interaction modes. *Nat. Cell Biol.* 17:530. http://dx.doi.org/10.1038/ncb3153

Kelly, A.E., S.C. Sampath, T.A. Maniar, E.M. Woo, B.T. Chait, and H. Funabiki. 2007. Chromosomal enrichment and activation of the Aurora B pathway are coupled to spatially regulate spindle assembly. *Dev. Cell.* 12:31–43. http://dx.doi.org/10.1016/j.devcel.2006.11.001

Kelly, A.E., C. Ghenoiu, J.Z. Xue, C. Zierhut, H. Kimura, and H. Funabiki. 2010. Survivin reads phosphorylated histone H3 threonine 3 to activate the mitotic kinase Aurora B. *Science.* 330:235–239. http://dx.doi.org/10.1126/science.1189505

Klein, U.R., E.A. Nigg, and U. Gruneberg. 2006. Centromere targeting of the chromosomal passenger complex requires a ternary subcomplex of Borealin, Survivin, and the N-terminal domain of INCENP. *Mol. Biol. Cell.* 17:2547–2558. http://dx.doi.org/10.1091/mbc.E05-12-1133

Lampson, M.A., K. Renduchitala, A. Khodjakov, and T.M. Kapoor. 2004. Correcting improper chromosome-spindle attachments during cell division. *Nat. Cell Biol.* 6:232–237. http://dx.doi.org/10.1038/ncb1102

Longtine, M.S., A. McKenzie III, D.J. Demarini, N.G. Shah, A. Wach, A. Brachat, P. Philippsen, and J.R. Pringle. 1998. Additional modules for versatile and economical PCR-based gene deletion and modification in *Saccharomyces cerevisiae*. *Yeast.* 14:953–961. http://dx.doi.org/10.1002/(SICI)1097-0061(199807)14:10<953::AID-YEA293>3.0.CO;2-U

Mackay, A.M., D.M. Eckley, C. Chue, and W.C. Earnshaw. 1993. Molecular analysis of the INCENPs (inner centromere proteins): separate domains are required for association with microtubules during interphase and with the central spindle during anaphase. *J. Cell Biol.* 123:373–385. http://dx.doi.org/10.1083/jcb.123.2.373

Makrantoni, V., S.J. Corbishley, N. Rachidi, N.A. Morrice, D.A. Robinson, and M.J.R. Stark. 2014. Phosphorylation of Sli15 by Ipl1 is important for proper CPC localization and chromosome stability in *Saccharomyces cerevisiae*. *PLoS One.* 9:e89399. http://dx.doi.org/10.1371/journal.pone.0089399

Muñoz-Barrera, M., and F. Monje-Casas. 2014. Increased Aurora B activity causes continuous disruption of kinetochore-microtubule attachments and spindle instability. *Proc. Natl. Acad. Sci. USA.* 111:E3996–E4005. http://dx.doi.org/10.1073/pnas.1408017111

Nakajima, Y., A. Cormier, R.G. Tyers, A. Pigula, Y. Peng, D.G. Drubin, and G. Barnes. 2011. Ipl1/Aurora-dependent phosphorylation of Sli15/INCENP regulates CPC-spindle interaction to ensure proper microtubule dynamics. *J. Cell Biol.* 194:137–153. http://dx.doi.org/10.1083/jcb.201009137

Nerusheva, O.O., S. Galander, J. Fernius, D. Kelly, and A.L. Marston. 2014. Tension-dependent removal of pericentromeric shugoshin is an indicator of sister chromosome biorientation. *Genes Dev.* 28:1291–1309. http://dx.doi.org/10.1101/gad.240291.114

Noujaim, M., S. Bechstedt, M. Wieczorek, and G.J. Brouhard. 2014. Microtubules accelerate the kinase activity of Aurora-B by a reduction in dimensionality. *PLoS One.* 9:e86786. http://dx.doi.org/10.1371/journal.pone.0086786

Peckham, M., and P.J. Knight. 2009. When a predicted coiled coil is really a single a-helix, in myosins and other proteins. *Soft Matter.* 5:2493–2503. http://dx.doi.org/10.1039/B822339D

Pereira, G., and E. Schiebel. 2003. Separase regulates INCENP-Aurora B anaphase spindle function through Cdc14. *Science.* 302:2120–2124. http://dx.doi.org/10.1126/science.1091936

Pinsky, B.A., C. Kung, K.M. Shokat, and S. Biggins. 2006. The Ipl1-Aurora protein kinase activates the spindle checkpoint by creating unattached kinetochores. *Nat. Cell Biol.* 8:78–83. http://dx.doi.org/10.1038/ncb1341

Samejima, K., M. Platani, M. Wolny, H. Ogawa, G. Vargiu, P.J. Knight, M. Peckham, and W.C. Earnshaw. 2015. The inner centromere protein (INCENP) coil is a single α-helix (SAH) domain that binds directly to microtubules and is important for chromosome passenger complex (CPC) localization and function in mitosis. *J. Biol. Chem.* 290:21460–21472. http://dx.doi.org/10.1074/jbc.M115.645317

Sandall, S., F. Severin, I.X. McLeod, J.R. Yates III, K. Oegema, A. Hyman, and A. Desai. 2006. A Bir1-Sli15 complex connects centromeres to microtubules and is required to sense kinetochore tension. *Cell.* 127:1179–1191. http://dx.doi.org/10.1016/j.cell.2006.09.049

Sarangapani, K.K., B. Akiyoshi, N.M. Duggan, S. Biggins, and C.L. Asbury. 2013. Phosphoregulation promotes release of kinetochores from dynamic microtubules via multiple mechanisms. *Proc. Natl. Acad. Sci. USA.* 110:7282–7287. http://dx.doi.org/10.1073/pnas.1220700110

Sessa, F., M. Mapelli, C. Ciferri, C. Tarricone, L.B. Areces, T.R. Schneider, P.T. Stukenberg, and A. Musacchio. 2005. Mechanism of Aurora B activation by INCENP and inhibition by hesperadin. *Mol. Cell.* 18:379–391. http://dx.doi.org/10.1016/j.molcel.2005.03.031

Storchová, Z., J.S. Becker, N. Talarek, S. Kögelsberger, and D. Pellman. 2011. Bub1, Sgo1, and Mps1 mediate a distinct pathway for chromosome biorientation in budding yeast. *Mol. Biol. Cell.* 22:1473–1485. http://dx.doi.org/10.1091/mbc.E10-08-0673

Tanaka, T.U., N. Rachidi, C. Janke, G. Pereira, M. Galova, E. Schiebel, M.J.R. Stark, and K. Nasmyth. 2002. Evidence that the Ipl1-Sli15 (Aurora kinase-INCENP) complex promotes chromosome bi-orientation by altering kinetochore-spindle pole connections. *Cell.* 108:317–329. http://dx.doi.org/10.1016/S0092-8674(02)00633-5

Tseng, B.S., L. Tan, T.M. Kapoor, and H. Funabiki. 2010. Dual detection of chromosomes and microtubules by the chromosomal passenger complex

drives spindle assembly. *Dev. Cell.* 18:903–912. http://dx.doi.org/10.1016/j.devcel.2010.05.018

Vader, G., J.J.W. Kauw, R.H. Medema, and S.M.A. Lens. 2006. Survivin mediates targeting of the chromosomal passenger complex to the centromere and midbody. *EMBO Rep.* 7:85–92. http://dx.doi.org/10.1038/sj.embor.7400562

Vader, G., C.W.A. Cruijsen, T. van Harn, M.J.M. Vromans, R.H. Medema, and S.M.A. Lens. 2007. The chromosomal passenger complex controls spindle checkpoint function independent from its role in correcting microtubule kinetochore interactions. *Mol. Biol. Cell.* 18:4553–4564. http://dx.doi.org/10.1091/mbc.E07-04-0328

van der Horst, A., and S.M.A. Lens. 2013. Cell division: control of the chromosomal passenger complex in time and space. *Chromosoma.* 123:25–42

van der Horst, A., M.J.M. Vromans, K. Bouwman, M.S. van der Waal, M.A. Hadders, and S.M.A. Lens. 2015. Inter-domain cooperation in INCENP promotes Aurora B relocation from centromeres to microtubules. *Cell Reports.* 12:380–387. http://dx.doi.org/10.1016/j.celrep.2015.06.038

Wang, F., J. Dai, J.R. Daum, E. Niedzialkowska, B. Banerjee, P.T. Stukenberg, G.J. Gorbsky, and J.M.G. Higgins. 2010. Histone H3 Thr-3 phosphorylation by Haspin positions Aurora B at centromeres in mitosis. *Science.* 330:231–235. http://dx.doi.org/10.1126/science.1189435

Yamagishi, Y., T. Honda, Y. Tanno, and Y. Watanabe. 2010. Two histone marks establish the inner centromere and chromosome bi-orientation. *Science.* 330:239–243. http://dx.doi.org/10.1126/science.1194498

Yue, Z., A. Carvalho, Z. Xu, X. Yuan, S. Cardinale, S. Ribeiro, F. Lai, H. Ogawa, E. Gudmundsdottir, R. Gassmann, et al. 2008. Deconstructing Survivin: comprehensive genetic analysis of Survivin function by conditional knockout in a vertebrate cell line. *J. Cell Biol.* 183:279–296. http://dx.doi.org/10.1083/jcb.200806118